



Rockfall susceptibility analysis of the “San Michele Arcangelo” historic trail (Central Italy) based on virtual outcrops and multiple propagation models

Luigi Guerriero¹ · Mariagiulia Annibali Corona¹ · Diego Di Martire¹ · Mirko Francioni² · Miriam Limongiello¹ · Rita Tufano¹ · Domenico Calcaterra¹

Received: 8 June 2023 / Accepted: 22 May 2024
© The Author(s) 2024

Abstract

The “San Michele Arcangelo” historic trail (Aurunci Regional Park, central Italy), located along the southern slope of Mt. Altino, which is highly prone to rockfalls, is hiked every year by thousands of faithful on pilgrimage who are exposed to such kinds of instabilities. To contribute to a better understanding of the condition and evolution of such phenomena, providing a susceptibility scenario able to support the adoption of mitigation measures, a specific analysis was completed based on field and literature data. Three-dimensional virtual outcrop models were obtained through both photogrammetric and iPad Pro LiDAR surveys to derive geomechanical features of outcropping rocks and estimate potential detaching block volume. Possible mechanisms of detachment were then analyzed using the Markland test method. Susceptibility to rockfall propagation and block deposition was analyzed using GIS processing and rockfall propagation simulations based on deterministic/stochastic models. Such models consist of a combination of a deterministic algorithm able to simulate the physics of rockfall movement during propagation and a stochastic treatment of input parameters based on random sampling within defined interval. Two different rockfall simulations were compared in this study using the Rockyfor3D™ (ecorisQ Association) software and the newly developed RocFall3© (RocScience) code. The use of iPad Pro LiDAR survey provides accurate and high-resolution point clouds, with high speed of acquisition and real-time processing of data. Discontinuity sets identified from 3D models have represented the input for kinematic analyses of slopes, allowing to identify potential failure mechanisms among wedge and planar sliding or toppling. Rockfall simulations indicate the potential for rock blocks propagation and deposition over the whole study area. Comparing the results of rockfall simulations with the geomorphological map of the area it is evident the control exerted by the hydrographic network on rockfall propagation as demonstrated by the presence of screes and slope deposits along the main channels. Understanding the potential susceptibility to both propagation and deposition of rock blocks along the trail provides useful indication for the assessment of appropriate mitigation measures to realize for the safer touristic fruition of the site.

Keywords Rockfall susceptibility analysis · Historic trail · iPad LiDAR · Markland test · Aurunci Regional Park · Virtual outcrop models

Introduction

Archaeological areas in hilly and mountainous regions of the world are seriously threatened by geological hazards (e.g. Pavlova et al. 2017; Valagussa et al. 2021; Tufano et al. 2022), and efforts are required to preserve cultural heritage in these regions. The Apennine mountains (Italy) are disseminated with many trekking trails, including forest tracks and remnants of ancient commercial roads, transhumance paths and religious trails (so called “cammini” and/or “tratturi”), now considered part of the cultural asset of the Apennine landscape. Due to their historic and cultural

✉ Rita Tufano
rita.tufano@unina.it

¹ Department of Earth, Environmental and Resource Sciences, Federico II University of Naples, Naples, Italy

² Department of Pure and Applied Sciences, Carlo Bo University of Urbino, Urbino, Marche, Italy

significance, such roads and trails are often hiked by visitors and tourists who, also as a consequence of the rapid development of the slow and cycle tourisms (Caffyn 2017; Gazzola et al. 2018), choose with increased frequency such locations for single or multiday trips. However, as a consequence of their mountainous nature, also related to the historic need of connecting remote locations (e.g. hermitages), such roads and trails often develop along slopes prone to landslides that, threatening visitors, prevent from a safe fruition of the asset. Interaction between landslides and hiking trails in the Cinque Terre National Park (Italy) has been studied by Raso et al. (2019), who assess the proneness of any single trail to be hit and damaged by landslides through the introduction of a Footpath Landslide Index. Di Luzio et al. (2020) present a study about the rockfall processes affecting a segment of the ancient Appia route in the central Apennines, built along a steep rock slope prone to rockfall with consequence for the ancient road track and unsafety conditions for the visitors. Giordan et al. (2020) focus on geo-hydrological instabilities affecting the “Sentiero Verde-Azzurro” trail, again in the Cinque Terre National Park.

Due to their sudden nature, rockfall events are among the most harmful phenomena for the human life in mountainous area (Corominas et al. 2014). Under these conditions, a susceptibility analysis is always recommended to localize critical zones for rock block detachments and propagations and for supporting risk analysis and mitigation strategies (Corominas et al. 2014). Landslide susceptibility can be assessed through either qualitative or quantitative methods, generally depending on the available datasets and methods that are used (Briones-Bitar et al. 2020). Qualitative analyses are mostly expert-based and susceptibility scenarios are prepared on the basis of geomorphologic field interpretations. Quantitative analyses are often based on data-driven statistical methods or physically-based methods. Rockfall susceptibility is often assessed using quantitative approaches: GIS-based statistical analyses are often preferred over large areas (Guzzetti et al. 2003; Frattini et al. 2008; Samodra et al. 2016; Messenzehl et al. 2017; De Stefano et al. 2021), while geomechanical analyses associated to physically-based propagation models are preferred for slope-scale analyses (Matasci et al. 2018). With the increase of digital mapping and spatial modeling tools (e.g. Guerriero et al. 2020), three-dimensional combined deterministic – probabilistic rockfall simulation models are widely used in rockfall issues, at both local and regional scale (Dorren et al. 2006). The difficult determination of rock blocks rebound can represent a limitation of these techniques, which usually use coefficients of energy loss (i.e. coefficients of restitution) derived from literature data, or randomly varied within a given distribution. Slope surface roughness is another critical parameter, generally set on the base of rock radius and size of slope material.

Recent developments in Terrestrial Laser Scanning (TLS), ground-based and unmanned aerial vehicle (UAV) photogrammetry have complemented the rockfall susceptibility analysis supporting geomechanical survey of slopes, especially in absence of minimum safety condition (Riquelme et al. 2015, 2018; Francioni et al. 2020; Rodriguez et al. 2020). Such methods are consistently used also in archaeological site analysis and restoration as well as in case of landslides affecting cultural heritage sites (Pappalardo et al. 2016; Mineo and Pappalardo 2020; Confuorto et al. 2021). Emerging sophisticated sensors and enhanced augmented reality, allow partial or complete automation of the modeling process, so it is possible to obtain accurate and in a near-real time 3D reconstructions. An example is represented by iPad Pro and the iPhone 12 Pro LiDAR-based virtual outcrop models. Spreafico et al. (2021) and Tavani et al. (2022) have shown that iPad Pro and iPhone 12 Pro LiDAR sensors are generally feasible and achieve accurate and precise measurements with efficient labor effort compared to conventional approaches, representing an interesting novelty also thanks to its cost (compared to standard surveying instruments), portability and limited time required both for data acquisition and processing. Another important aspect is that this technology is only slightly affected by lighting conditions, differently to the traditional photogrammetry (Gollob et al. 2021). On the other hand, Łabędź et al. (2022) demonstrate that models obtained by the iPad Pro LiDAR sensors strongly depend on the sampling frequency and grid size. Moreover, the potential application of this technique is severely constrained by its maximum range of 5 m, which greatly limits the size of objects that can be acquired, but the versatility of these instruments outweighs the range limitation, making these LiDAR devices a very valuable economic alternative among remote sensing techniques (Luetzenburg et al. 2021). With the aim of improving the geomechanical field studies, photogrammetric surveys can be sided to LiDAR devices.

In this paper, susceptibility to rockfall of the “San Michele Arcangelo” historic trail, in the Aurunci Regional Park of Italy, is evaluated through i) geomechanical analysis conducted through field survey and 3D modeling aided by both photogrammetry and iPad Pro LiDAR surveys and virtual outcrop models generation, ii) kinematic analysis, iii) GIS processing and rockfall propagation and deposition simulations. Such simulations have been undertaken using the GIS-based Rockyfor3D™ software and the newly developed RocFall3© with the goal to highlight advantages and limitations of the two codes. Rockyfor3D™ software is based on a rigid body approach which considers rock blocks dimension randomly varying in a predefined percentage for each simulation; slope surface roughness is considered by an obstacle height (MOH), randomly chosen from the value predetermined by the user and according to their probabilities of

occurrence (Li and Lan 2015). RocFall3© is a 3D statistical analysis program which consists of both lumped mass and rigid body analysis methods. The lumped mass model includes impact and sliding physics, whereas the rigid body engine has a sphere impact model. Both lumped mass and rigid body physics engines can scale the coefficient of restitution (R_n) by velocity and mass. Comparison between these two software is done in this work for the first time, determining energy, velocity, and bounce heights of rock blocks along multiple rock paths. In addition, the significance of the study is related to the characteristics of the “San Michele Arcangelo” historic trail, an example of historic trail of great religious significance that, every year, is hiked by thousands of faithful on pilgrimage (Fig. 1). It develops for 7.3 km along the southern slope of Mt. Altino, a mountainside particularly prone to rockfalls due to its geological and geomorphological characteristics. Representing a significant threaten to human life for the site, since 2018, the historic trail was closed to visitors by local authorities due to the need for a new and updated susceptibility assessment to support risk mitigation measures planning. The assessment of failure type and rockfall mechanisms in the area of the “San Michele Arcangelo” historic trail provides new insights into rockfall susceptibility of the site as well as into transit and deposition scenario of rock blocks, useful to support risk analysis and mitigation measures adoption in view of a safer fruition of the historic trail.

Study area

The study area comprises a sector of the southern slope of Mt. Altino (1365.7 m a.s.l.), in the Aurunci Regional Park (central Italy). Stratigraphic setting of the study area consists

of a pre-orogenic succession of Mesozoic carbonates from the Latium-Abruzzi platform Auct (*sensu* Chiocchini and Mancinelli 1977), which includes limestones and dolomites; recent slope deposits are locally present (Fig. 2). The structural setting consists of a deformed fold belt, ENE–WSW oriented and bounded to N–E by a main thrust fault (Latina Valley Thrust Front), while Plio–Pleistocene normal faults offset towards S–E the whole structure (Rossi et al. 2002; Tallini and Parotto 2013). Contractional structures, dated early Messinian to upper Tortonian and NNW–SSE oriented, dissect the carbonate range of Aurunci Mts. (Di Luzio et al. 2020). As a consequence, rocks cropping out in the study area are consistently characterized by multiple discontinuity sets and locally carbonate limestones are overlaid by calcareous-marly limestones as observed during field survey. This condition could increase proneness to rock slope instability related to a change of rock properties. As well, rock block detachment can be also linked to the slightly variable bedding trend in relation to the presence of multiple folds, as indicated by block deposits at specific locations of the slope (screes; Fig. 3).

Recent slope deposits are concentrated next to slope-parallel creeks and below major scarps characterizing the upper sector of the slope to form screes (Fig. 3). They mostly consist of rockfall blocks, characterized by a volume between 0.1 and 0.2 m³, and talus deposits, and appear to be associated with isolated blocks located at different elevations along the slope (Fig. 3). A fraction of such isolated blocks appears to have significant dimensions (volume > 0.5 m³) as those locally observed along the historic trail (Fig. 4).

The “San Michele Arcangelo” historic trail, conducting to the namesake hermitage, crosses the study area from east to west following the convergent catchment morphology of the slope (Fig. 3). As observable in Fig. 3, the trail consists

Fig. 1 Map showing the study area including the “San Michele Arcangelo” historic trail developed along the southern slope of Mt. Altino in the Aurunci Regional Park. Significant assets, like the trail and the hermitage, and locations are reported in the map. The letters a, b, c, d, e and f indicate the position in which the photos in Fig. 4 were captured. Inset map depicts the position of the study area within the Italian territory

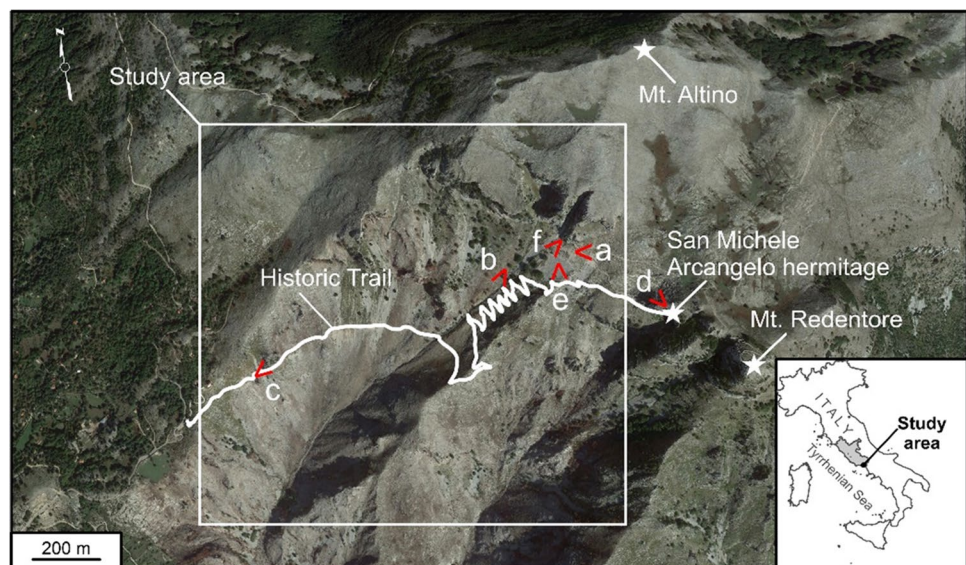


Fig. 2 Geological map of the study area (modified from ISPRA geological map, Sheet 171, Scale 1:100000 – Bergomi et al. 1969). 1) continental and marine deposits (Holocene-Upper Pleistocene); 2) syn-orogenic siliciclastic deposits (Upper-Middle Miocene); 3) Liguride Unit basinal deposits (Lower Miocene-Oligocene); 4) carbonate platform deposits (Paleocene-Jurassic); 5) carbonate platform deposits (Lower Jurassic-Upper Triassic); 6) fault; 7) inferred fault

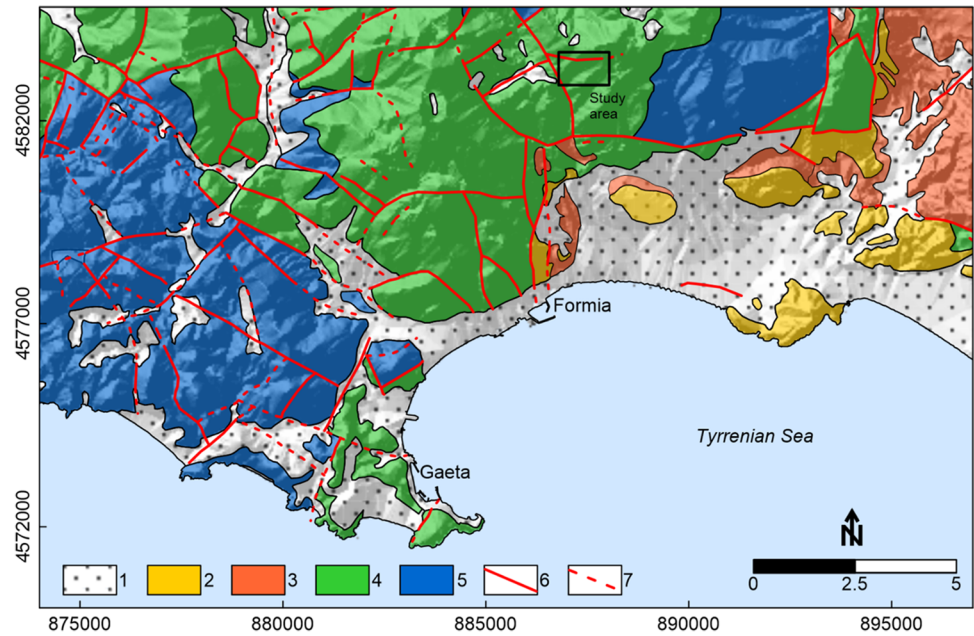
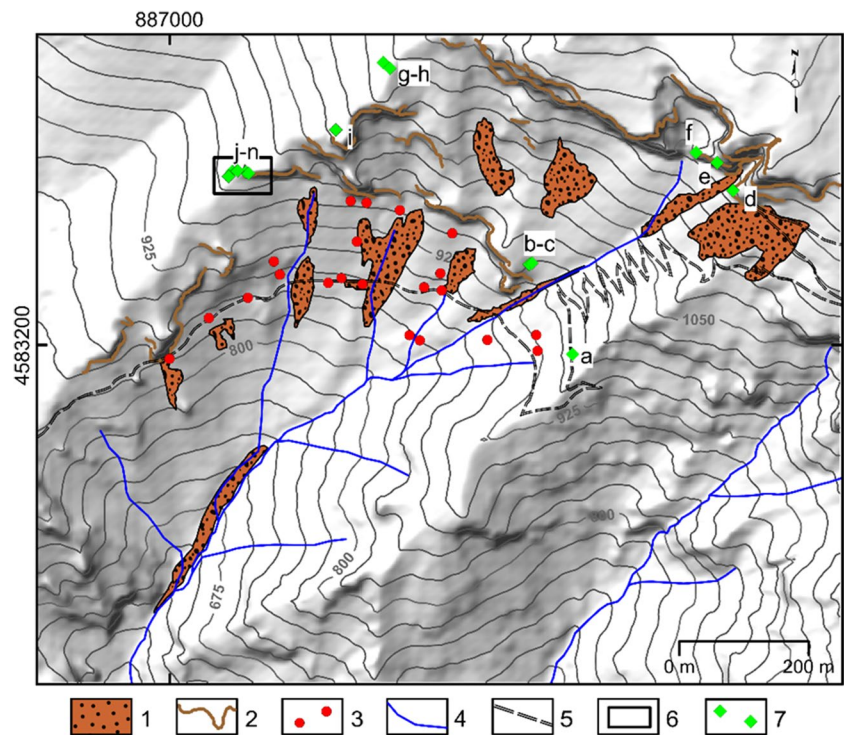


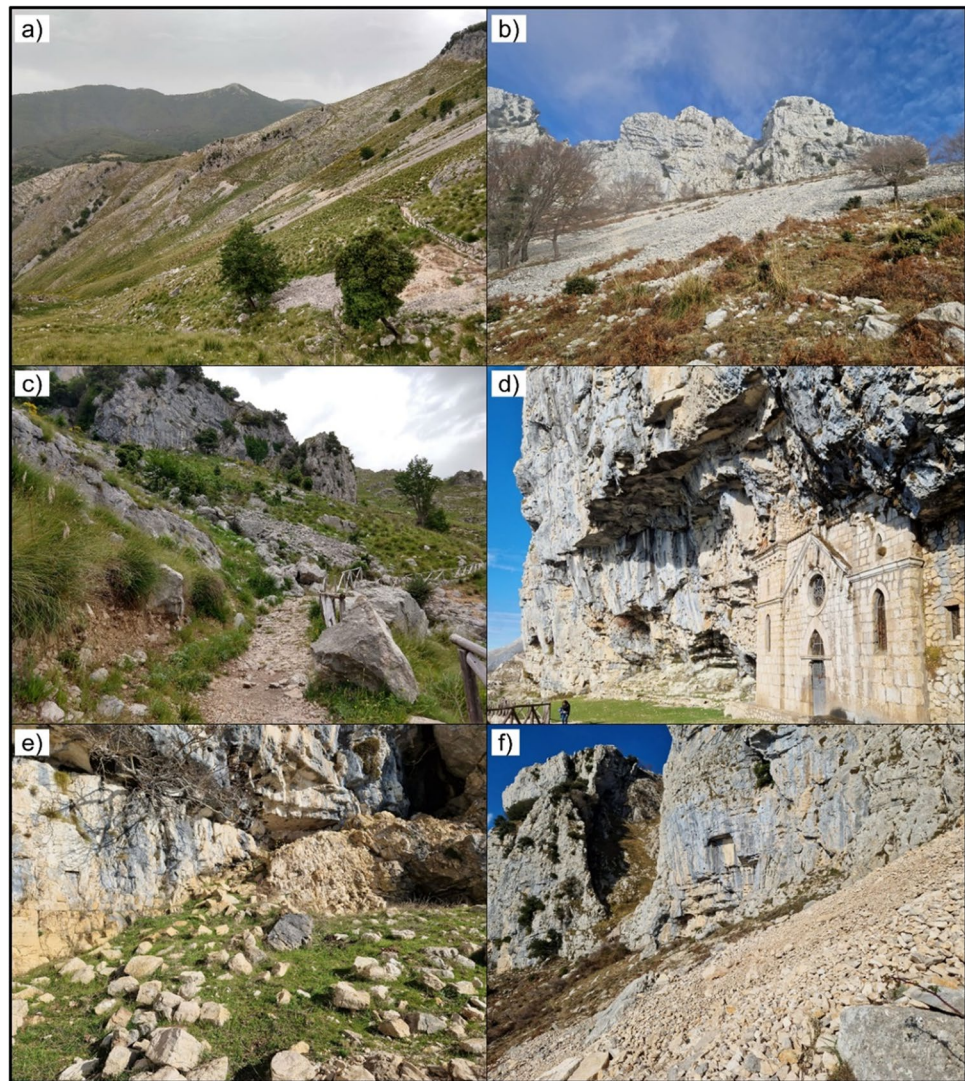
Fig. 3 Geomorphologic map of the study area. 1) Scree; 2) Scarp; 3) Boulder; 4) Hydrograph network; 5) “San Michele Arcangelo” historic trail; 6) Surveyed area with terrestrial photogrammetric method; 7) Area surveyed with iPad LiDAR, conventionally indicated by letters from *a* to *n*. UTM 32 N – WGS84 coordinates are shown at map edges



of two segments: a first one crossing the whole catchment at an elevation ranging between 805 and 925 m a.s.l., and a second segment developed in the western sector of the catchment from an elevation of 925 m to 1060 m a.s.l.. Figure 4a and b provide an overview of the morphology of the first segment

of the trail, while Fig. 4c shows how the trail appears along its course. Figure 4d shows the “San Michele Arcangelo” hermitage. Figures 4e and f highlight the variation in dip of bedding as well as the presence of discontinuity sets which pervade the outcropping rocks and generate rock blocks of variable volume.

Fig. 4 Pictures showing a) western side of the “San Michele Arcangelo” historic trail; b) rocky scarp and scree; c) portion of the “San Michele Arcangelo” historic trail with rock blocks detached from the upper sector of the slope; d) the “San Michele Arcangelo” hermitage and the rocky outcrop that lies above it; e) rocky scarp showing the contact between calcareous and calcareous-marly limestones; f) details on discontinuities pervading rocky scarps which result in rock blocks of variable volume. Position of the pictures are shown in Fig. 1



Methods

Ground-based photogrammetric survey

Terrestrial photogrammetric survey using a conventional technique has been carried out to reconstruct the 3D model of an accessible sector of the southern slope of Mt. Altino. The position of the surveyed area is presented in Fig. 3. Photogrammetric reconstruction as well as geomechanical and structural analyses were carried out by means of ShapeMetrix 3D (©3GSM GmbH) software using the Structure from Motion approach (SfM). SfM is a method of photogrammetry that allows the reconstruction of high-resolution 3D models using multiple images without needing to set Ground Control Points (GCP). Digital photogrammetry has been applied to a number of geological problems, including discontinuity characterization (Krosley et al. 2006; Sturzenegger and Stead 2009) and rock slope stability analysis (Haneberg 2008; Francioni et al. 2019; Mineo

and Pappalardo 2020; Albarelli et al. 2021; Confuorto et al. 2021). This approach has been chosen because it is able to perform analyses on the basis of slope morphological features and with a limited presence of vegetation.

The photogrammetric technique allows for reconstructing objects in the form of three-dimensional point clouds starting from two-dimensional image sets (Westoby et al. 2012; Galantucci and Fatiguso 2019). To obtain a uniform coverage of the area, it is necessary, during the acquisition phase, to maximize the overlap by adopting short baselines. Along with ShapeMetrix 3D software, a Canon EOS 80D camera equipped with a factory calibrated lens characterized by a focal length of 10 mm has been provided by the producers and used for the survey. In this work, pictures were taken considering the position of materialized GCPs, which in the SfM approach allow the refinement process through calculations based on the projection matrix of every single image (Luhmann et al. 2016). Pictures were taken keeping a consistent orientation of the camera toward the slope and

an approximate height from the ground of approximately 1.50 m. A total of 85 frames were acquired for the selected slope sector considering a minimum normal distance of 3 m from the front and a longitudinal acquisition step of approximately 1 m; by doing so, an approximately 80% overlap was reached. The acquisition of the photos was completed during a particularly bright time of the day, avoiding shadow zones to maximize model quality.

ShapeMetrix 3D photogrammetry software was used to complete the 3D field site reconstruction and structural analysis. The reconstruction of the 3D model has been accomplished using all of the acquired frames and the SMX - Multi Photo tool, based on the SfM approach. Such a tool allows for position reconstruction of each single frame (Image Alignment), coarse point cloud reconstruction and dense point cloud generation. For model georeferencing, GNSS coordinates of individual twelve specifically materialized GCPs were measured in the field through the Real-Time Kinematics (RTK) technique. A RTK calibrated surveyor kit provided by ArduSimple was used for the survey, reaching an average accuracy in positioning of GCPs of ± 0.02 m.

iPad pro LiDAR survey

To derive geomechanical data over the whole study area, increasing the representativeness of discontinuity measurements of the structural setting, a total of 14 iPad Pro LiDAR-based surveys have been carried out at eight accessible locations, as reported in Fig. 3. The iPad Pro 6th generation

(Apple Inc.) runs with iOS 16.4.1 and is equipped with a LiDAR module and associated high resolution camera. The scanning app used for surveys is the 3D Scanner App. During the surveys, the devices was maintained in a steady, slow pace walking and the distance between the sensor and the outcropping scarp within 1.50 m. Horizontal and vertical movements along the main axis of the device perpendicular to the scanned surfaces has been allowed to acquire the dense point clouds in a few minutes. After acquisition the raw point cloud is automatically postprocessed for quality and a final point cloud is derived. The dense point clouds obtained has been imported in CloudCompare v.2.13. (examples are shown in Fig. 5) to derive high resolution virtual outcrop models by point cloud meshing. Virtual outcrop models are subsequently used for discontinuity measurements and sets and relating spacing identification.

Discontinuity detection

The structural and geomechanical analysis of the slope model derived by the photogrammetric survey has been carried out using a plug-in of ShapeMetriX 3D named JMS - Analyst tool. It allows for generation of geometric measurements directly into 3D models, so that each recognized feature can be analyzed using point normal or trace measurements. A trace measurement is a polygonal line that follows the surface of the object in a 3D space; its length is given along the surface in terms of Euclidean distance. Traces are also used to determine the spacing of a set of structures. The

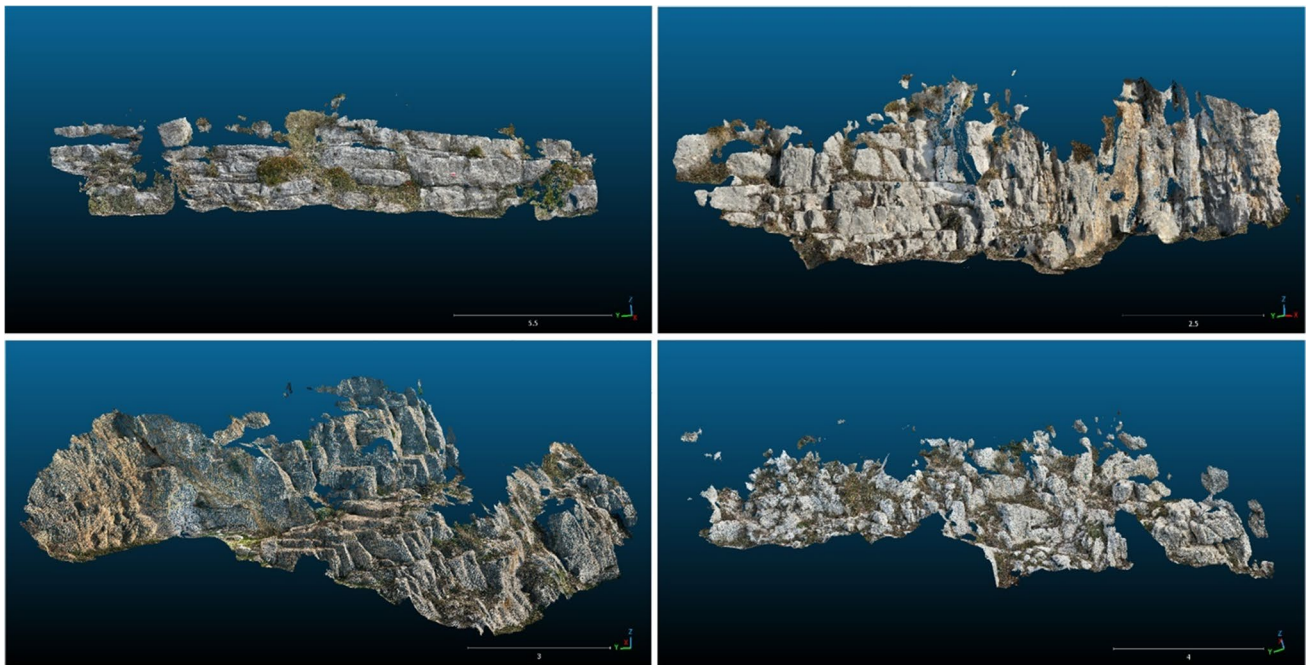


Fig. 5 Pictures showing some examples of dense point clouds obtained by iPad LiDAR imported in CloudCompare software

JMS Analyst plug-in allows for grouping the measurements into sets, with automatic clustering and stereographic/statistical projections. Annotations like length of the drawn track, dip and dip direction values and position in terms of X, Y, Z, are automatically grouped within the identified discontinuity sets (DS). Thus, once parameterized through the definition of cluster number (in this case, four) the analysis provides different sets of rock mass discontinuities. This method is semiautomatic with the possibility of validation, which was performed by comparison with local field measurements.

Discontinuity detection on the basis of virtual outcrop models derived by iPad Pro LiDAR-based surveys has been carried out in an interactive way through the CloudCompare v2.13. plug-in Compass. Compass is a structural geology toolbox for the interpretation and analysis of virtual outcrop models. It contains several tools for measuring orientations, among these the plane tool has been used in this analysis to measure the orientations of fully exposed planar surfaces (i.e. joint and bedding surfaces) and the trace tool which allows the estimation of discontinuity contact's orientation based on its intersection with a non-flat surface. Clustering analysis has been subsequently conducted using *Stereonet* v.11 software.

Finally, the rock block volume V_b , representing the equivalent volume of potentially detaching blocks, was estimated with the method commonly used when are present more than one discontinuity set, as follows (Palmstrom 2005):

$$V_b = S_a^3 \quad (1)$$

where S_a identifies the average spacing of the discontinuity sets, generally estimated through the following relation:

$$S_a = (S1 + S2 + S3 + \dots Sn)/n \quad (2)$$

where S1, S2 and Sn are the measured spacing, characterizing each identified discontinuity set.

Kinematic analysis

Data obtained from structural analysis have been used as a basis for a Markland (1972) oriented to the definition of the stability characteristics of the slope in terms of detachment potential. Due to large number of discontinuities, only representative orientation values (dip/dip direction) for DSs identified by means of the clustering analysis have been considered. For the slope face orientation, the presence of slope faces oriented from N140° to N320°, from the western to the eastern sector of the study basin, allowed to consider different slope orientations for the surveys carried out. Since rockfall susceptibility is somehow related to slope angle, for this analysis the maximum observed inclination of approximately 80° was considered as reference value. A friction angle of 35° has been considered on the basis of

literature data for materials forming the slope (Singh and Goel 2011). Analysis of the angular relationships between the representative value of orientation for each discontinuity set and the slope surface (Kliche 1999) was completed through the software *Stereonet* v.11 to identify the potential for block detachment and related modes of failures among wedge sliding, planar siding and non-flexural toppling.

Rockfall simulation

Rockyfor3D™ and RocFall3© based propagation analyses have been completed for estimating susceptibility to rockfall propagation and block deposition and for comparing and highlighting advantage and limitations of the two codes.

Rockyfor3D™ calculates trajectories of single falling rock block with defined geometry in three dimensions (3D). In this software the input parameters (i.e. release location, density, shape and dimensions of rock blocks, local slope surface roughness and coefficient of restitution R_n) are assigned to the digital surface through GIS processing according to field observations and/or digital elevation data. The release locations have been identified on the base of the Markland test results and GIS processing of the DEM considering sectors of the study area characterized by a slope angle higher than 50°; rock density has been set according to literature as 2500 kg/m³ (Di Luzio and Carfora 2018; Di Luzio et al. 2020). Block volume was defined according to the estimated block size (Eq. 1) and block geometry was considered rectangular according to field observations. Overall, the simulations were completed considering a volume of 0.30 m³ ± 20%. The number of rock blocks for each simulation step is 100 for each grid cell which is considered as starting point of falling. About the local slope surface roughness, it is represented by a parameter defined as maximum obstacle height (MOH). Typical values of this parameter, as suggested by Dorren and Simoni (2014), which are encountered by a falling rock are represented by statistical classes, namely rg70%, rg20%, and rg10%. Due to the presence of rockfall deposits and talus, in this case the local surface roughness has been considered only for slope sectors characterized by the presence of screes. By means of field measurement of relative height of asperities from the ground, rg70%, rg20%, and rg10% were defined for value of 0.15, 0.20 and 0.35, respectively. Finally, R_n , the parameter determining energy loss during a rebound on the surface, has been set according to Dorren et al. (2006).

RocFall3© is instead not a GIS based software and allows the user to perform both Lumped Mass and Rigid Body rockfall analyses. Geometry of slopes has been imported from DEM, while the input parameters have been assigned directly in the software interface. Specifically, the parameters release locations, rock density and block shape have been set equal to those used for Rockyfor3D™ simulation,

while the normal coefficient of restitution R_n , here defined as the negative ratio of the outgoing velocity to incoming velocity, has been set equal to 0.315 for the detachment area and 0.32 for the scree area. Finally, the dynamic friction coefficient (μ), the parameter that control the dissipation of rock energy during rockfall was assigned equal to 0.7 for the area of outcropping bedrock and 0.5 for the screes assigned using the RocScience 2023 guidelines (RocScience 2023).

For both the analyses, a single sided 5 m pixel dimension DEM, resampled from 1 m LiDAR-derived DEM (<http://www.pcn.minambiente.it/mattm/progetto-pst-dati-lidar>), was used to represent surface topography. Due to the spacing of discontinuities that reaches the maximum value of about 1 m, pixel dimension of the DEM was set greater than the maximum dimension of a possible rock block. In this way, such a DEM was also used as a basis for deriving potential detachment zones, needed for the propagation analysis. Satellite orthophotos were managed in GIS environment and used to develop the soil cover map and, in particular, the scree areas.

Results

Point clouds and structural features of the slope

Processing of the frames acquired with ground-based photogrammetry allowed for creation of a 3D model of the selected slope sector located next to the watershed (see Fig. 3 for position). A dense point cloud consisting of more than 500,000 points, with a point spacing of ~ 0.04 m and a point density of ~ 558 sample/m², has been generated

with only local gaps due to the presence of vegetation. Figure 6 provides an overview of the dense points cloud and its interpretations in terms of identified and measured discontinuities.

Overall, 41 discontinuities were identified from interactive model examinations and 3 discontinuity sets (DSs), besides the bedding (S), were recognized by cluster analysis (different colors of arrows in Fig. 6 indicate the discontinuity sets). Discontinuities geometries, in terms of dip-direction and dip-angle, are shown in Fig. 7a. Figure 7b shows the Fisher concentration of identified discontinuities allowing to isolate major clusters and related DSs. Table 1 reports representative orientation for each discontinuity set. Dip-direction of DSs variates from 324° (DS1) to 215° (S), while dip varies between 30° (S) and 84° (DS2). Discontinuity spacing, measured during the field survey and the interactive model examinations, varies between 0.4 and 1 m. Such orientation data are consistent with field measurements of discontinuities completed at accessible locations identified along the historic trail for validation purposes (Table 1). In addition, field observation of discontinuity planes indicated how their surfaces are moderately rough and weakly altered and systems with lower real spacing appear to be recemented.

Starting from discontinuity data, including their spacing, block volume was estimated (Table 2) and compared with that observed during field analyses. The calculation of the block size returned a S_a of ~ 0.7 m and a V_b of ~ 0.35 m³.

Surveys conducted using the iPad Pro LiDAR sensors provide 3D models representative of different area of the basin: the *a* survey for the western part, from *b* to *f* surveys for the central and upper part, and from *g* to *n* for the east part, next to the watershed (see Fig. 3). Number of points,

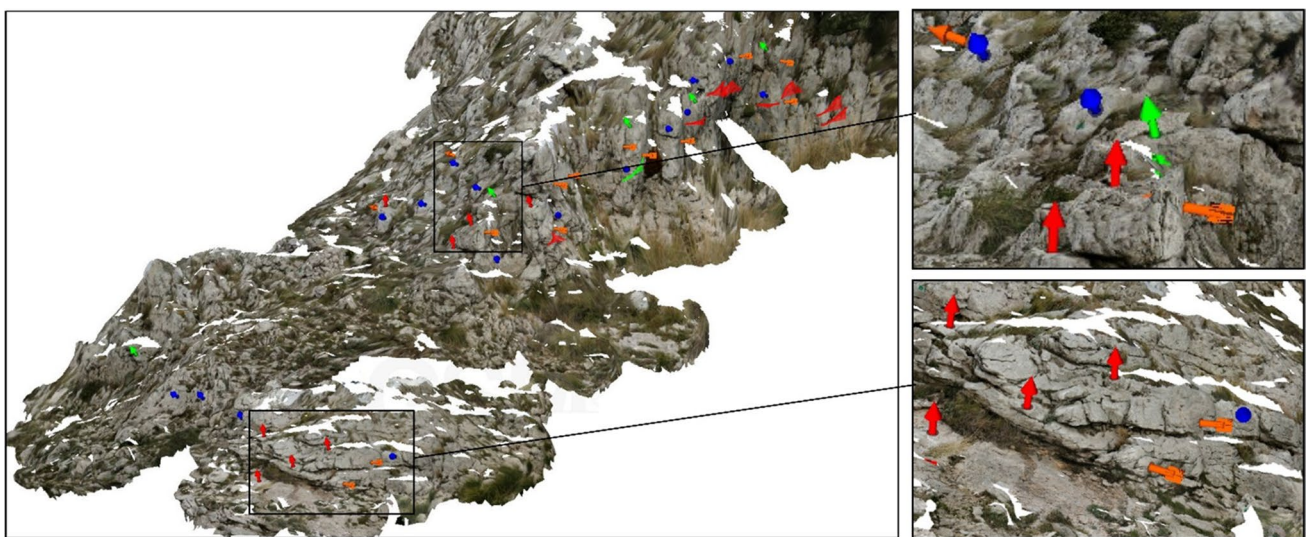


Fig. 6 Dense point cloud derived by ground-based image processing. Colors of arrows represent different discontinuity sets (DSs): DS1) orange; DS2) blue; DS3) green; S) red. A fraction of detected discontinuities is indicated as normal to planes and line features

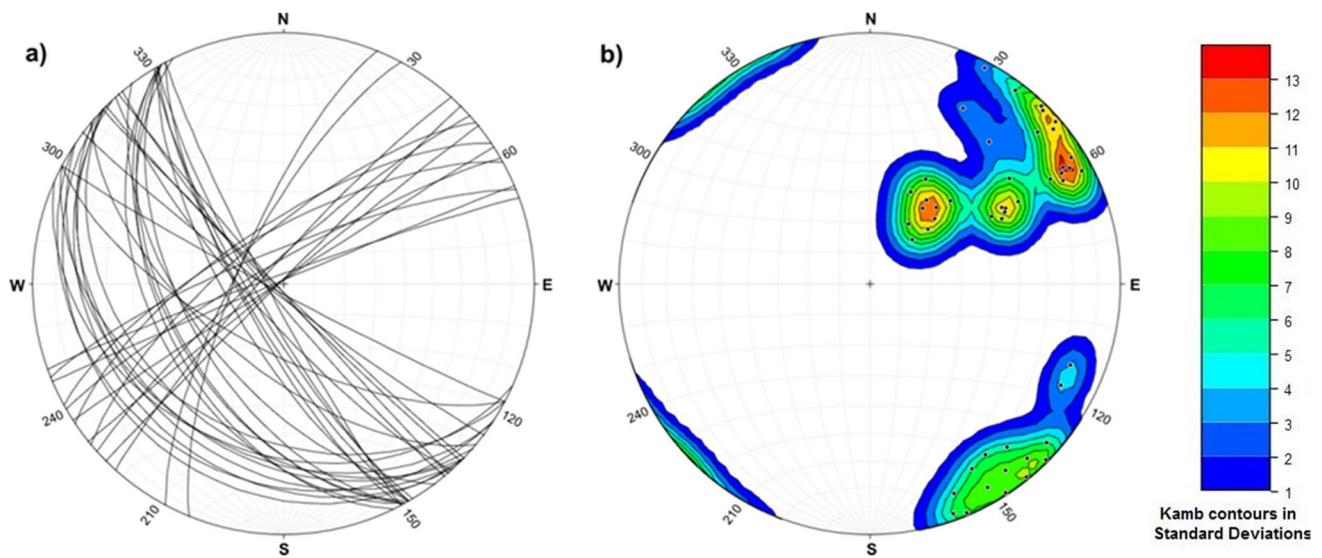


Fig. 7 Plot showing discontinuities identified through interactive model examination (a) and measurement and clustering analysis of discontinuities (b)

Table 1 Discontinuity sets identified through clustering analysis in photogrammetric model and field survey. S=bedding

Discontinuity set (DS)	Photogrammetric model		Field survey	
	Dip-direction (°)	Dip-angle (°)	Dip-direction (°)	Dip-angle (°)
DS1	324	81	318	80
DS2	238	84	220	80
DS3	242	51	235	55
S	215	30	200	32

Table 2 Average, minimum and maximum spacing identified for each discontinuity set (DS). S=bedding

Discontinuity set (DS)	Average spacing (m)	Min spacing (m)	Max spacing (m)
DS1	1.12	0.85	1.37
DS2	0.62	0.42	0.89
DS3	0.78	0.58	0.95
S	0.39	0.22	0.78

Table 3 Characteristics of the dense point clouds derived by surveys conducted using the iPad Pro LiDAR sensors

Survey	N. points	Point spacing (m)	Point density (samples/m ²)	N. discontinuities
a	848,100	0.006	26,214	26
b	391,267	0.007	20,402	31
c	558,164	0.006	27,557	26
d	404,016	0.006	32,144	30
e	663,348	0.006	23,814	63
f	556,836	0.005	43,588	55
g	1,016,525	0.006	25,132	44
h	709,330	0.007	20,097	38
i	290,437	0.006	29,038	35
j	862,661	0.007	17,360	48
k	433,889	0.005	40,179	37
l	433,954	0.005	40,116	37
m	536,004	0.007	20,372	25
n	249,528	0.008	15,133	24

spacing and density of LiDAR extracted point clouds are reported in Table 3. Also in this case, few gaps in the models are present due to the presence of vegetation (Fig. 5). The interactive model examination conducted in CloudCompare environment allowed to identify a variable number of discontinuities, from 24 for the *m* survey to 63 for the *e* survey (Table 3).

During the identification of the DSs, because of their proximity, the models related to survey *b – c*, *e – f*, *g – h*

and *j – n* were merged, obtaining a total of seven stereonets (Fig. 8). In almost all the cases, four DSs, including the bedding *S*, have been recognized. Only in the cases of *b–c* and *i* surveys three DSs including *S*, have been identified from the cluster analysis. Table 4 summarizes the representative orientation for each DSs as well as the spacing measurements, interactively carried out for the block size estimation.

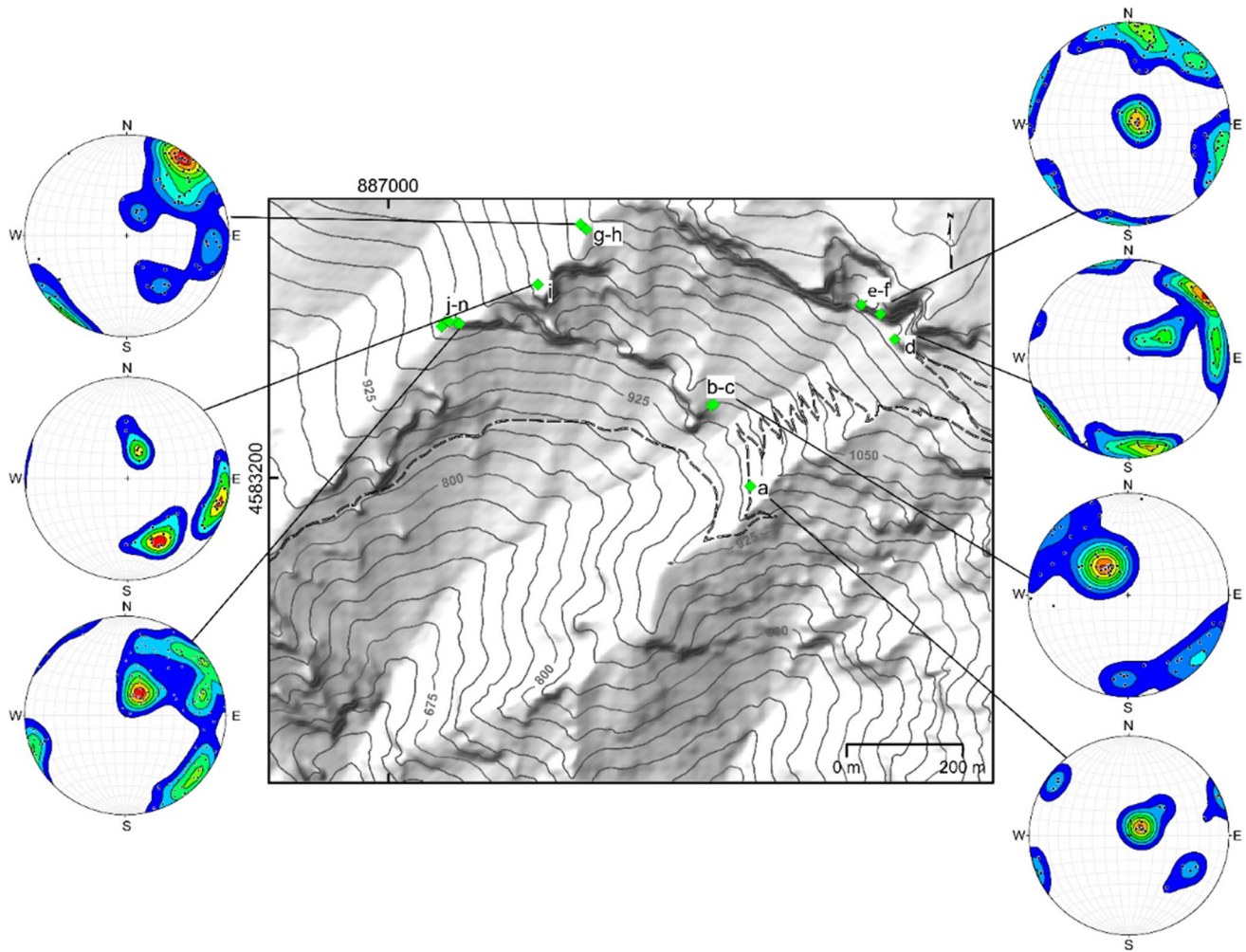


Fig. 8 Plots showing discontinuities identified through interactive model examination and clustering analysis of discontinuities for each area surveyed with iPad LiDAR indicated in the map

Failure mechanisms analysis and rockfall susceptibility

Figures 9 and 10 show the results from the Markland test which points out the potential types of failures that can occur in the study area. In particular, Fig. 9 shows the Markland test carried out using photogrammetry data and the three different slope orientations (N140°, N190° and N230°) measured in the field. For slope sectors with orientation N140° (Fig. 9a) potential toppling can occur on the basis of the orientation of DS1 (T1; Fig. 9a). In slope sectors with N190° orientation, the intersection between discontinuity sets DS1 and DS3 creates conditions for wedge failures (W1; Fig. 9b). In slope sectors with N230° orientation, discontinuity set DS3 has the potential to develop planar sliding (S1; Fig. 9c) and discontinuity sets DS1 and DS3 create conditions for wedge failures (W1; Fig. 9c).

Figure 10 shows the results from the Markland test for the DSs identified through the iPad LiDAR-based virtual outcrop models analysis. For the considered slope orientations, in almost all cases different types of failures can occur. The most unfavorable condition occurs for the survey *d* and slope orientation of 320° (*d*, 320° of Fig. 10) for which DS1 has the potential to promote planar sliding (S1), while the intersections of DS1-DS3 and DS2-DS3 create conditions for wedge failure (W1 and W2).

Results from the structural analysis and field observations allowed to derive relevant input parameters for rockfall susceptibility analysis in terms of detachment, propagation and deposition areas. According to the Markland test results, all the investigated rock outcrops could be affected by rock failures. Therefore, slopes with angles higher than 50° have been classified during the rockfall analysis as potential rockfall source areas. Such area has been identified through GIS

Table 4 Characteristic orientation of the DSs identified through clustering analysis for the surveys *a, b-c, d, e-f, g-h, i, j-n*. S=bedding

Survey	Discontinuity set (DS)	Dip-direction (°)	Dip-angle (°)	Average spacing (m)	Block volume (m ³)
<i>a</i>	DS1	339	85	0.97	0.31
	DS2	215	88	0.40	
	DS3	219	59	0.78	
	S	158	11	0.57	
<i>b - c</i>	DS1	311	86	0.45	0.38
	DS2	—	—	—	
	DS3	004	70	0.86	
	S	150	30	0.87	
<i>d</i>	DS1	337	83	0.76	0.23
	DS2	237	87	0.74	
	DS3	252	78	0.22	
	S	220	22	0.71	
<i>e - f</i>	DS1	297	88	0.23	0.15
	DS2	227	80	0.42	
	DS3	193	77	0.56	
	S	236	17	0.89	
<i>g - h</i>	DS1	326	56	0.87	0.35
	DS2	215	82	0.51	
	DS3	276	77	1.02	
	S	216	19	0.42	
<i>i</i>	DS1	333	63	1.06	0.24
	DS2	284	83	0.38	
	DS3	—	—	—	
	S	202	23	0.43	
<i>j - n</i>	DS1	313	85	1.02	0.34
	DS2	247	80	0.50	
	DS3	235	65	0.86	
	S	207	29	0.45	

processing of the DEM, which allows for estimation of the susceptibility to detachment. Rockyfor3D™ and RocFall3© simulations permitted instead to determine susceptibility to propagation and deposition over the study area and, in particular, the simulations provided distributed estimation of i) distribution of stopping points indicative of susceptibility to deposition; ii) maximum heights from the ground of moving blocks during propagation; iii) maximum kinetic energy; iv) maximum speed.

Distribution of detachment areas of Fig. 3, as well as distribution of screes and overall slope characteristics were considered during the definition of restitution coefficient. In particular, in the simulation carried out with Rockyfor3D™, following indication from Dorren et al. (2006), an Rn value of 0.53 was assigned to detachment areas characterized by outcropping bedrock, Rn equal to 0.38 to screes, formed by coarse sediments and boulders, and Rn equal to 0.43 to the slope, characterized by outcropping bedrock locally covered by fine sediments (Table 5). In this way, slope areas with varying substrate characteristics contribute in a differentiated manner to downslope rock block propagation. Regarding the analysis with RocFall3©, Rn values were assigned starting by RocScience 2023 guidelines and following a calibration phase based on a trial-and-error approach. The best values obtained are 0.315 and 0.32 for outcropping bedrock and scree, respectively (Table 5).

The results of the simulation can be observed in Figs. 11a-b and 12a-f. In particular, Figs. 11a-b shows the susceptibility map gathered from Rockyfor3D™ and the End-point map from RocFall3©. It is possible to see that maps highlight important similarities with the local conditions as reported by the geomorphological map of the study area (Fig. 3) and especially in relation to rock-fall deposition susceptibility which is generally low in

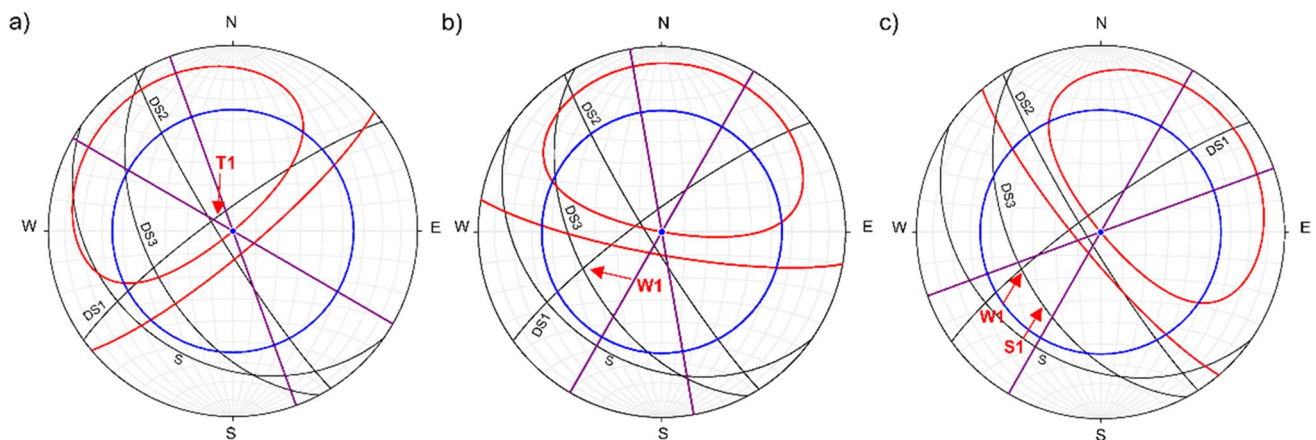


Fig. 9 Markland test stereographic projections carried out using photogrammetry data. Discontinuity sets are reported using planes (gray lines). Large blue circles represent friction angle ($\phi = 35^\circ$). Slope face and slope direction limits are reported using red and magenta colors,

respectively. T1 indicates conditions for potential toppling instability, S1 for potential planar sliding and W1 for potential wedge formation. Slope orientation: a) N140°, b) N190°, c) N230°

Fig. 10 Markland test stereographic projections carried out using iPad LiDAR virtual outcrop models. Discontinuity sets are reported using planes (gray lines). Large blue circles represent friction angle ($\phi = 35^\circ$). Slope face and slope direction limits are reported using red and magenta colors respectively. T1 indicates conditions for potential toppling instability, S1 for potential planar sliding and W1 and W2 for potential wedge formation. For each plot, surveys and slope orientation are reported

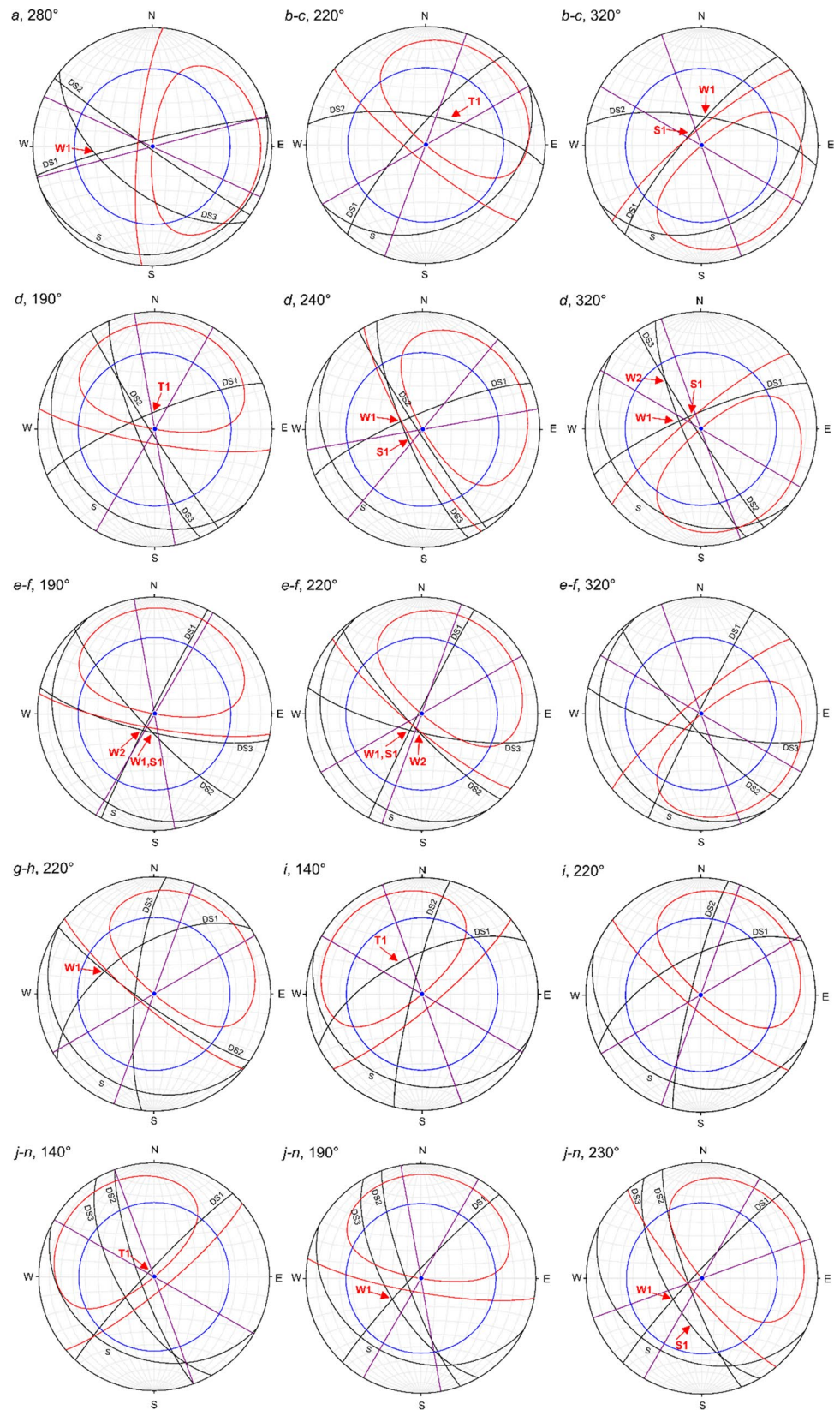


Table 5 Restitution coefficients characterizing the study area as estimated following Dorren et al. (2006) for Rockyfor3D™ and RocScience 2023 guidelines for RocFall3©

Zone	Rn	
	Rockyfor3D™	RocFall3©
Detachment area	0.53	0.315
Scree	0.38	0.32
Slope	0.43	–

the upper and medium sectors of the analyzed slope and higher on the scree areas. Moreover, the hydrographic network exerts an evident control on rock removal in the main channel as demonstrated by the presence of an important block deposition in the simulation results, less evident in the geomorphological map.

Figures 12a-c illustrate the findings from Rockyfor3D™ analysis in terms of rockfall velocity, kinetic energy and bouncing height maps. Figures 12d-f highlight the same maps from the RocFall3© simulations. The maximum velocity has been found to be values around 35÷40 m/s in both the analyses and have been recorded, as expected, in proximity of the steepest slope angles (Figs. 12a-d). After detachment, blocks undergo a consistent acceleration as a consequence of slope morphometry. During rockfalls, a kinetic energy ranging between 600 and 1300 KJ has been calculated along the trail. Also in this case, a good correspondence between the two simulations (Figs. 12b-d) has been obtained. Bouncing height along the trail varies between few to ca. 10/15 m in both the simulations.

Discussion

Thanks to the advent of terrestrial laser scanners on the one hand and high-resolution cameras, sometimes mounted on unmanned aerial vehicles, on the other one, the use of photogrammetric techniques has remarkably improved in recent years. The use of these techniques becomes even more important when dealing with non-accessible and/or unsafe areas. Sarro et al. (2018) and Konstantinidis et al. (2021) illustrated the use of unmanned aerial vehicle-based photogrammetry for rockfall analysis in cultural heritage areas, while Francioni et al. (2019) demonstrated the potentiality of hand-held cameras in the engineering characterizations of rock slopes.

In the last two decades, data derived from LiDAR (Light Detection And Ranging) technology has been widely employed for supporting geomechanical surveys of slopes. To increasingly facilitate digital geological fieldwork using accurate high-resolution data acquisition and high geo-location accuracy, LiDAR sensors have been recently implemented in mobile devices, such as iPhones and iPads (Luetzenburg et al. 2021; Tavani et al. 2022). In geological applications, such implementation can be useful to reconstruct, in near-real time, 3D virtual outcrop models which allow the detection of structural discontinuities of the rock masses.

In this research, both ground-based photogrammetry methodology and iPad LiDAR sensors have been used to carry out 3D virtual outcrop models of sectors of the southern slope of Mt. Altino and to improve data gathered from geomechanical surveys. The choice of using a 3D model interactive structural analysis was motivated by the unsafe accessibility of rock outcrops. Considering the characteristics of the analyzed slope, the use of these techniques has

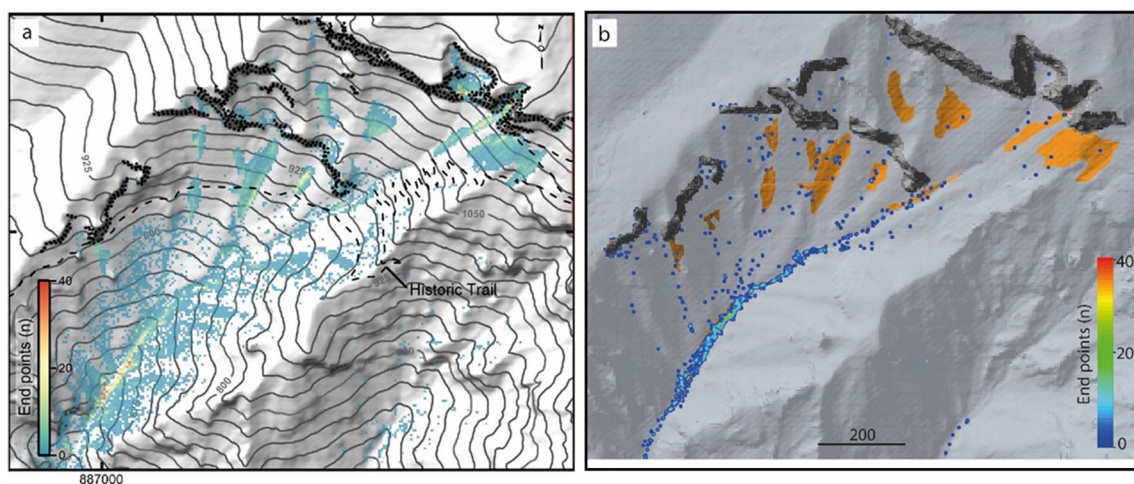


Fig. 11 Distribution of areas identified as susceptible to blocks deposition in Rockyfor3D™ (a) and RocFall3© (b) simulations

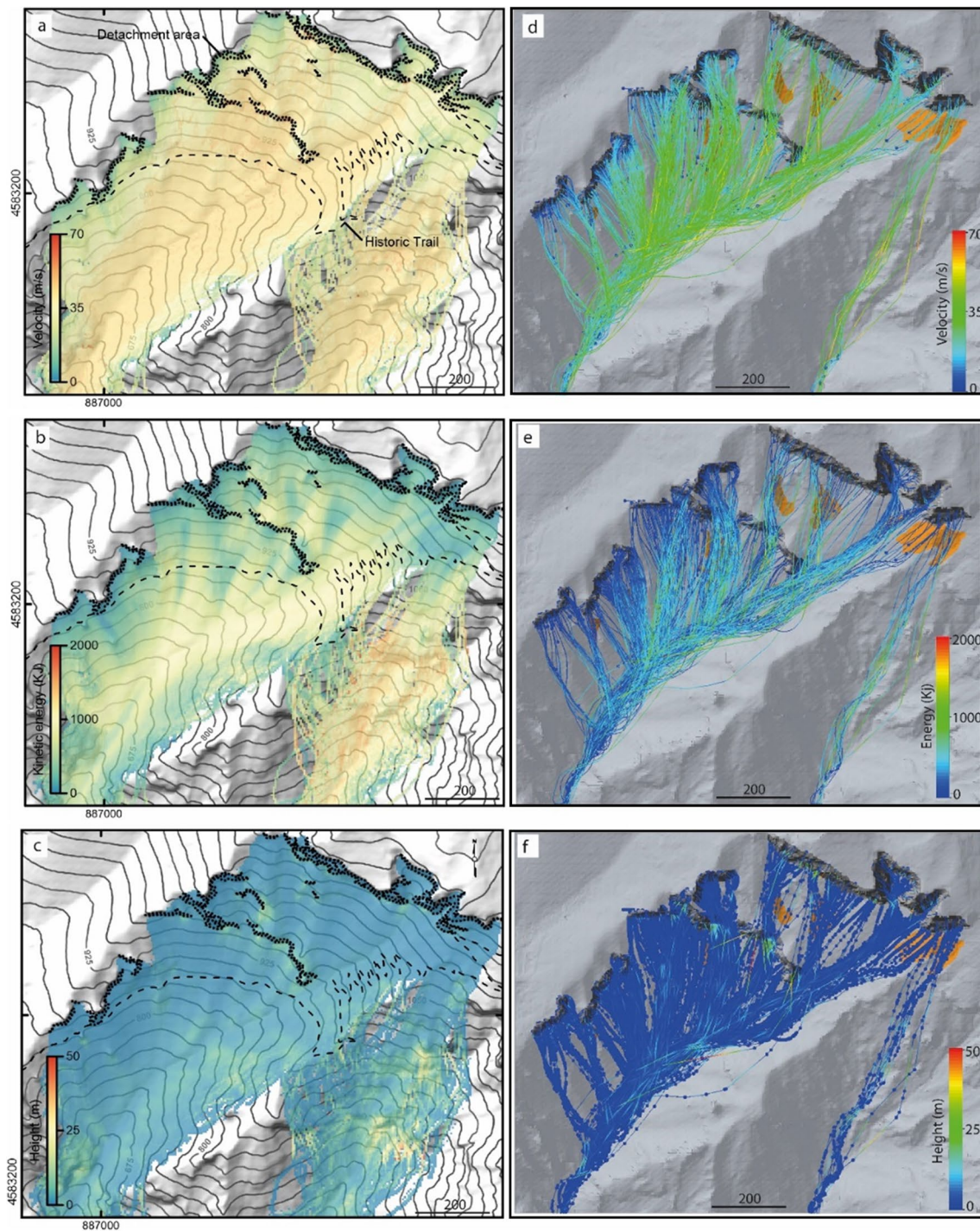


Fig. 12 Rockyfor3D™ simulation results in terms of maximum velocity (a), maximum kinetic energy (b), maximum height (c). RocFall3© simulation results in terms of maximum velocity (d), maximum kinetic energy (e), maximum height (f)

allowed to conduct, in safe conditions, a survey and analysis of discontinuity sets, maximizing the representativeness of the acquired data.

The combination of photogrammetric and iPad LiDAR data was important in defining the main joint sets characterizing the areas and their geomechanical characteristics,

including rock block volumes. The great amount of data provided by the acquisition conducted through the iPad allowed an extensive scanning of representative sectors of the study area for DSs identification. Comparison between the orientation of identified DSs in the j - n surveys and the photogrammetric survey, shows a good correspondence

between iPad LiDAR and ground-based photogrammetric survey's data. Data derived by virtual outcrop models analysis indicate a dip-direction of S varies from 150° and 236° , while dip varies between 11° and 30° , probably due to the blandly folds which affect the outcropping rocks (Fig. 13a, b), according to field measurements and the results of model derived by photogrammetric survey (only for data abtained form *j-n* surveys). Also spacing measuraments, interactively carried out for the block size estimation, are in agreement with those measured during field and photogrammetric surveys, even if a reduced block volume can be recognizable for surveys *d* and *e-f*, probably due to the presence of the marly limestones with more pervasive fractures. Such estimations appear to be consistent with rock blocks located along the trail and forming screes (Fig. 14a, b). Exceptions are represented by isolated large blocks characterized by an estimated volume greater than 0.5 m^3 . Differences between volume estimated from

discontinuity analysis and locally observed larger blocks can be related to local heterogeneities in rock masses fabric.

The Markland test highlights the primary role of slope orientation for instability conditions in the study area and identifies the eastern sector of Mt. Altino as the area most susceptible to rock block detachment due to the presence of multiple westward cliff segments. This observation is supported by the distribution of screes in the study area, located consistently below westward cliff segments (Fig. 3). Moreover, the presence of the calcareous-marly limestone cropping out in the top area of basin, can be linked to the most unfavorable conditions for which the intersection of DSs is responsible of mostly wedge and planar failures. Even if a certain variability in the dip-direction and dip-angle exists, especially for DS3, the same failure mechanisms can be recognized for the slope orientation of 140° , 190° and 230° . Such results demonstrate the valuable contribution that

Fig. 13 Pictures of outcrop rocks affected by blandly folds (a, b), determining locally changes in the bedding orientation

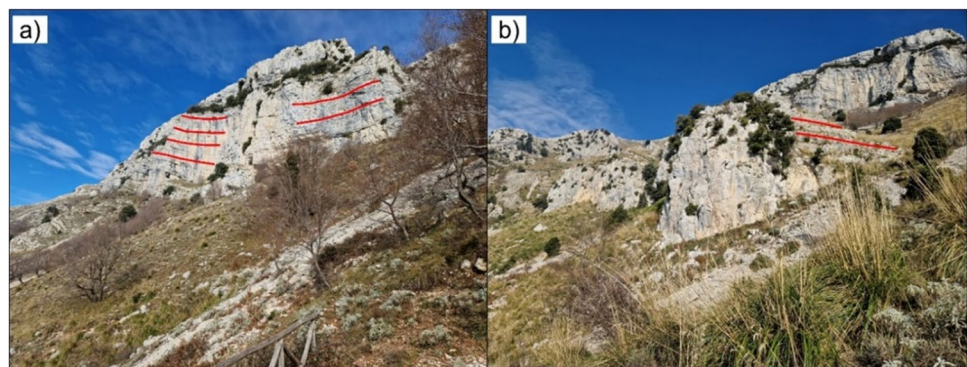
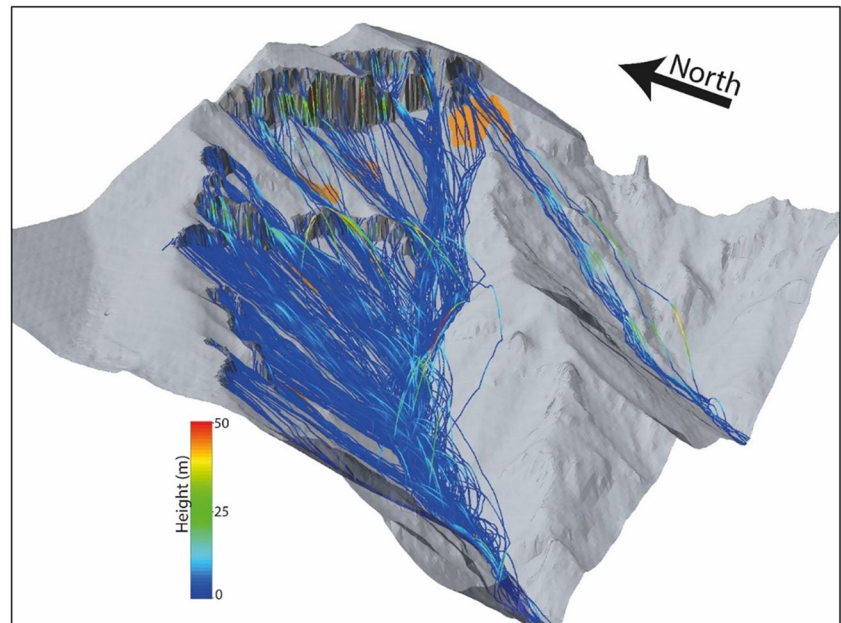


Fig. 14 Rock blocks along the trail and forming screes (a, b)



Fig. 15 Three-dimensional visualization of rockfall bouncing in RockFall3



LiDAR sensors implemented on mobile devices can give in solving slope stability problems.

The use of GIS in rockfall simulation problems plays an important role in the study of wide areas. In the case studied, indeed, thematic maps can be extracted to improve the geomorphological interpretation of the area and soil cover. Through the combined use of thematic maps, orthophotos and information from field surveys, it was possible to develop the base model for rockfall simulation and define the local slope roughness and Rn coefficient. A similar approach has been documented in literature when rockfall analysis has to be conducted over wide areas (Schober et al. 2012; Corona et al. 2017; Francioni et al. 2020; Noël et al. 2021).

Finally, maps obtained by the two rockfall simulation software, compared in this study, highlight a very similar result with a good correspondence of the area interested by rockfall propagation and rock block deposition. In fact, if Rockyfor3D™ is a well-known code used in rockfall simulations by several authors through the years (Dorren et al. 2004; Corona et al. 2017; Francioni et al. 2019; Moos et al. 2019; Robiati et al. 2019), application of the newly developed software RocFall3© based on the previous 2D version, RocFall2, are very few in the literature yet. Due to the recent advent of this code, its comparison with a well-known and tested software (i.e. Rockyfor3D™) represents an interesting analysis to highlight its potential advantages and limitations. The use of different Rn values for the same slope zone (Table 5), according to Dorren et al. (2006) for Rockyfor3D™ and RocScience 2023 guidelines for RocFall3©, indicates some differences between the two codes but also poses the attention on a right calibration phase preparatory to modeling. The data visualization for the two code is also

different. Rockyfor3D™, being a GIS-based software, offers the possibility to visualize the results in GIS environment. In this case, although the analysis is three-dimensional, the results are expressed through pixel color maps. RocFall3© uses a different approach, where the rockfall simulation can be visualized in terms of rockfall bouncing: an example of this process is reported in Fig. 15, where the three-dimensional visualization of rockfall bouncing is illustrated. This offers the advantage to better understand and interpret the rockfall risk in the different slope areas. On the other hand, Rockyfor3D™ allows for developing personalized GIS maps where it is possible to highlight more information (e.g. Figures 13 and 14 highlight the possibility to locate the trail in the Rockyfor3D™ simulation). Although RocFall3© does not offer this possibility, it is possible to visualize the results on top of aerial/satellite photographs and/or thematic maps (RocScience, 2023).

Conclusions

The preservation and protection of natural sites has always been a topic much investigated by both the scientific community and land management entities (Evans 1975; Harmon and Kyle 2022). The objective is twofold, on the one hand to safeguard what can be defined as geosites (Calcaterra et al. 2014), in terms of biodiversity and geological peculiarities, and on the other hand to improve the use by hikers and increase naturalistic awareness. In this context, the "San Michele Arcangelo" trail represents an example of historic trail of great religious significance, and it is considered an important touristic asset for the Lazio Region of Italy. The trail is located along the southern slope of Mt. Altino characterized by several rockfall susceptible areas, with steepness

up to 70–80°, representing a risk for tourists and pilgrims. In this context, to contribute to a better understanding of rockfall initiation and propagation conditions in the area of the "San Michele Arcangelo" historic and providing a susceptibility scenario able to support the adoption of mitigation measures, a specific analysis was completed on the basis of field and literature data. Three discontinuity sets and the bedding have been detected from the virtual outcrop models, with orientation slightly variable relating to geological structures (i.e. folds) which affect the study area. Intersection between DSs and slope orientation are also responsible of instability conditions, especially in the eastern sector of Mt. Altino along the multiple westward cliff segments.

Advantages in the use of virtual outcrop models derived through iPad LiDAR technologies were extensively stressed in the paper, representing a useful solution for accurate and high-resolution data in view of new fieldwork technologies development especially for unsafe accessibility of locations. Moreover, data provided by such models have been allowed to detect potential mechanisms of detachment using the Markland test method and have represented a support for estimating specific parameters for susceptibility analysis. Finally, the use of the two codes for rockfall propagation and deposition simulations, Rockyfor3D™ and RocFall3©, and the comparison of results poses the attention on the need for a right calibration phase of such estimated parameters.

Considering the high landscape value of the trail studied, possible landslide risk mitigation measures may be designed and dimensioned based on results of rockfall propagation and rock block deposition simulations.

Supplementary Information The online version contains supplementary material available at <https://doi.org/10.1007/s10064-024-03764-0>.

Acknowledgments The authors thank Consorzio interUniversitario per la prevenzione dei Grandi Rischi (CUGRI) for providing technological support. Also, we thank Benedetto Casale for his support in field work and photogrammetric model interpretations.

Funding Open access funding provided by Università degli Studi di Napoli Federico II within the CRUI-CARE Agreement. This research was funded by "Convenzione per l'affidamento di uno studio geologico-tecnico e geomeccanico relativo alle condizioni di stabilità dei versanti nell'area del sentiero storico religioso San Michele Arcangelo nel Comune di Formia (LT), Parco Naturale Regionale dei Monti Aurunci", Principal Investigator: D. Calcaterra, Scientific coordinator: L. Guerriero, and by AIM Project, grant number AIM18352321 – 1.

Declarations

Conflict of interest The authors declare no conflict of interest.

Open Access This article is licensed under a Creative Commons Attribution 4.0 International License, which permits use, sharing, adaptation, distribution and reproduction in any medium or format, as long as you give appropriate credit to the original author(s) and the source, provide a link to the Creative Commons licence, and indicate if changes were made. The images or other third party material in this article are

included in the article's Creative Commons licence, unless indicated otherwise in a credit line to the material. If material is not included in the article's Creative Commons licence and your intended use is not permitted by statutory regulation or exceeds the permitted use, you will need to obtain permission directly from the copyright holder. To view a copy of this licence, visit <http://creativecommons.org/licenses/by/4.0/>.

References

- Albarelli DSNA, Mavrouli OC, Nyktas P (2021) Identification of potential rockfall sources using UAV-derived point cloud. *Bull Eng Geol Environ* 80:6539–6561. <https://doi.org/10.1007/s10064-021-02306-2>
- Bergomi C, Catenacci C, Cestari G, Manfredini M, Manganelli V (1969) Note illustrative alla Carta Geologica d'Italia alla scala 1:100000, foglio 171: Gaeta e vulcano di Roccamonfina. Servizio Geologico Italiano
- Briones-Bitar J, Carrión-Mero P, Montalván-Burbano N, Morante-Carballo F (2020) Rockfall research: a bibliometric analysis and future trends. *Geosciences* 10(403):1–25. <https://doi.org/10.3390/geosciences10100403>
- Caffyn A (2017) Slow tourism. Special interest tourism: concepts, contexts and cases. CAB International, Wallingford, pp 183–195. <https://doi.org/10.1079/9781780645667.0183>
- Calcaterra D, Guida D, Budetta P, De Vita P, Di Martire D, Aloia A (2014) Moving geosites: how landslides can become focal points in Geoparks. In: Latest trends in engineering mechanics, structures, engineering geology, Proceedings of the 7th International Conference on Engineering Mechanics, Structures, Engineering Geology (EMESEG 14) Salerno, Italy, pp 162–171
- Confuorto P, Di Martire D, Longo M, Vicario EI, Calcaterra D (2021) Rockfall susceptibility assessment for the preservation of archaeological sites in the Amalfi coast (southern Italy) by using UAV photogrammetry. In: 13th landslides and engineered slopes. Experience, theory and practice, SCG-XIII international symposium on landslides. Cartagena, Colombia
- Chiocchini M, Mancinelli A (1977) Microbiostratigrafia del Mesozoico in facies di piattaforma carbonatica dei Monti Aurunci (Lazio meridionale). *Studi Geol Camerti* 3:109–152 In Italian
- Corominas J, van Westen C, Frattini P, Cascini L, Malet JP, Fotopoulou S, Catani F, Van Den Eeckhaut M, Mavrouli O, Agliardi F, Pitilakis K, Winter MG, Pastor M, Ferlisi S, Tofani V, Hervás J, Smith JT (2014) Recommendations for the quantitative analysis of landslide risk. *Bull Eng Geol Environ* 73:209–263. <https://doi.org/10.1007/s10064-013-0538-8>
- Corona C, Lopez-Saez J, Favillier A, Mainieri R, Eckert N, Trappmann D, Stoffel M, Bourrier F, Berger F (2017) Modeling rockfall frequency and bounce height from three-dimensional simulation process models and growth disturbances in submontane broad-leaved trees. *Geomorphology* 281:66–77. <https://doi.org/10.1016/j.geomorph.2016.12.019>
- De Stefano R, Repola L, Guerriero L, Iovane D, Morra V, Pagano F, Di Martire D (2021) Rockfall threatening Cumae archaeological site fruition (Phlegraean Fields Park—Naples). *Sustainability* 13(1390):1–15. <https://doi.org/10.3390/su13031390>
- Di Luzio E, Carfora P (2018) Geomorphological records of diachronous quarrying activities along the ancient Appia route at the Aurunci Mountain pass (Central Italy). *Geomorphology* 306:210–223. <https://doi.org/10.1016/j.geomorph.2018.01.016>
- Di Luzio E, Mazzanti P, Brunetti A, Baleani M (2020) Assessment of tectonic-controlled rock fall processes threatening the ancient Appia route at the Aurunci Mountain pass

- (Central Italy). *Nat Hazards* 102:909–937. <https://doi.org/10.1007/s11069-020-03939-4>
- Dorren LKA, Maier B, Putters US, Seijmonsbergen AC (2004) Combining field and modelling techniques to assess rockfall dynamics on a protection forest hillslope in the European Alps. *Geomorphology* 57:151–167. [https://doi.org/10.1016/S0169-555X\(03\)00100-4](https://doi.org/10.1016/S0169-555X(03)00100-4)
- Dorren LKA, Berger F, Putters US (2006) Real-size experiments and 3-D simulation of rockfall on forested and non-forested slopes. *Nat Hazards Earth Syst Sci* 6:145–153. <https://doi.org/10.5194/nhess-6-145-2006>
- Dorren L, Simoni S (2014) Rockyfor3D (V5.1) Descrizione trasparente del modello 3D di caduta massi. www.ecorisq.org
- Evans J (1975) Protection guidelines per a Natural Trail. CURA Resources Collection
- Francioni M, Stead D, Sciarra N, Calamita F (2019) A new approach for defining slope mass rating in heterogeneous sedimentary rocks using a combined remote sensing GIS approach. *Bull Eng Geol Environ* 78:4253–4274. <https://doi.org/10.1007/s10064-018-1396-1>
- Francioni M, Antonaci F, Sciarra N, Robiati C, Coggan J, Stead D, Calamita F (2020) Application of unmanned aerial vehicle data and discrete fracture network models for improved Rockfall simulations. *Remote Sens* 12(2053):1–28. <https://doi.org/10.3390/rs12122053>
- Frattini P, Crosta G, Carrara A, Agliardi F (2008) Assessment of rockfall susceptibility by integrating statistical and physically-based approaches. *Geomorphology* 94:419–437. <https://doi.org/10.1016/j.geomorph.2006.10.037>
- Galantucci RA, Fatiguso F (2019) Advanced damage detection techniques in historical buildings using digital photogrammetry and 3D surface analysis. *J Cult Herit* 36:51–62. <https://doi.org/10.1016/j.culher.2018.09.014>
- Gazzola P, Pavione E, Grechi D, Ossola P (2018) Cycle tourism as a driver for the sustainable development of little-known or remote territories: the experience of the Apennine regions of northern Italy. *Sustainability* 10(1863):1–19. <https://doi.org/10.3390/su10061863>
- Giordan D, Cignetti M, Godone D, Peruccacci S, Raso E, Pepe G, Calcaterra D, Cevasco A, Firpo M, Scarpellini P, Gnone M (2020) A new procedure for an effective Management of geo-Hydrological Risks across the “Sentiero Verde-Azzurro” trail, cinque Terre National Park, Liguria (North-Western Italy). *Sustainability* 12(561):1–20. <https://doi.org/10.3390/su12020561>
- Gollob C, Ritter T, Kraßnitz R, Tockner A, Nothdurft A (2021) Measurement of Forest inventory parameters with apple iPad pro and integrated LiDAR technology. *Remote Sens* 13(3129):1–35. <https://doi.org/10.3390/rs13163129>
- Guerriero L, Di Martire D, Calcaterra D, Francioni M (2020) Digital image correlation of Google earth images for Earth’s surface displacement estimation. *Remote sensing*, 12(21), 3518, 1–14. <https://doi.org/10.3390/rs12213518>
- Guzzetti F, Reichenbach P, Cardinali M et al (2003) The impact of landslides in the Umbria region, Central Italy. *Nat Hazards Earth Syst Sci* 3:469–486. <https://doi.org/10.5194/nhess-3-469-2003>
- Haneberg WC (2008) Elevation errors in a LIDAR digital elevation model of West Seattle and their effects on slope-stability calculations. *Landslides and engineering geology of the Seattle, Washington, area*, rex L. Baum, Jonathan W. Godt, Lynn M Highland. [https://doi.org/10.1130/2008.4020\(03\)](https://doi.org/10.1130/2008.4020(03))
- Harmon J, Kyle G (2022) Connecting to the trail: natural spaces as places of healing. *Leis Sci* 44:1112–1127. <https://doi.org/10.1080/01490400.2020.1712282>
- Kliche CA (1999) Rock slope stability, 2nd edn. Society for Mining, Metallurgy, and Exploration Press. United States, Englewood
- Konstantinidis I, Marinos V, Papanthassiou G (2021) UAV-based evaluation of Rockfall Hazard in the cultural heritage area of Kipinas monastery, Greece. *Appl Sci* 11(8946):1–33. <https://doi.org/10.3390/app11198946>
- Krosley, L., Shaffner, P., Oerter, E., Ortiz, T., 2006, Digital ground-based photogrammetry for measuring discontinuity orientations in steep rock exposures., 41st U.S. Symposium on rock mechanics 9 (USRMS), Golden, Colorado
- Łabędź P, Skabek K, Ozimek P, Rola D, Ozimek A, Ostrowska K (2022) Accuracy verification of surface models of architectural objects from the iPad LiDAR in the context of photogrammetry methods. *Sensors* 22(8504):1–19. <https://doi.org/10.3390/s22218504>
- Li L, Lan H (2015) Probabilistic modeling of rockfall trajectories: a review. *Bull Eng Geol Environ* 74:1163–1176. <https://doi.org/10.1007/s10064-015-0718-9>
- Luetzenburg G, Kroon A, Bjørk AA (2021) Evaluation of the apple iPhone 12 pro LiDAR for an application in geosciences. *Sci Rep* 11(22221):1–9. <https://doi.org/10.1038/s41598-021-01763-9>
- Luhmann T, Fraser C, Maas H-G (2016) Sensor modelling and camera calibration for close-range photogrammetry. *ISPRS J Photogramm Remote Sens* 115:37–46. <https://doi.org/10.1016/j.isprsjprs.2015.10.006>
- Markland J (1972) A useful technique for estimating the stability of rock slopes when the rigid wedge slide type of failure is expected. Interdepartmental Rock Mechanics Project, Imperial College of Science and Technology
- Matasci B, Stock GM, Jaboyedoff M, Carrea D, Collins BD, Guérin A, Matasci G, Ravanel L (2018) Assessing rockfall susceptibility in steep and overhanging slopes using three-dimensional analysis of failure mechanisms. *Landslides* 15:859–878. <https://doi.org/10.1007/s10346-017-0911-y>
- Messenzehl K, Meyer H, Otto JC, Hoffmann T, Dikau R (2017) Regional-scale controls on the spatial activity of rockfalls (Turtmann Valley, Swiss Alps) — a multivariate modeling approach. *Geomorphology* 287:29–45. <https://doi.org/10.1016/j.geomorph.2016.01.008>
- Mineo S, Pappalardo G (2020) Sustainable fruition of cultural heritage in areas affected by Rockfalls. *Sustainability* 12(296):1–17. <https://doi.org/10.3390/su12010296>
- Moos C, Toe D, Bourrier F, Knüsel S, Stoffel M, Dorren L (2019) Assessing the effect of invasive tree species on rockfall risk – the case of *Ailanthus altissima*. *Ecol Eng* 131:63–72. <https://doi.org/10.1016/j.ecoleng.2019.03.001>
- Noël F, Cloutier C, Jaboyedoff M, Locat J (2021) Impact-detection algorithm that uses point clouds as topographic inputs for 3D Rockfall simulations. *Geosciences* 11(188):1–35. <https://doi.org/10.3390/geosciences11050188>
- Palmstrom A (2005) Measurements of and correlations between block size and rock quality designation (RQD). *Tunn Undergr Space Technol* 20:362–377. <https://doi.org/10.1016/j.tust.2005.01.005>
- Pappalardo G, Imposa S, Mineo S, Grassi S (2016) Evaluation of the stability of a rock cliff by means of geophysical and geomechanical surveys in a cultural heritage site (South-Eastern Sicily). *Ital J Geosci* 135:308–323. <https://doi.org/10.3301/IJG.2015.31>
- Pavlova I, Makrigakis A, Depret T, Jomelli V (2017) Global overview of the geological hazard exposure and disaster risk awareness at world heritage sites. *J Cult Herit* 28:151–157. <https://doi.org/10.1016/j.culher.2015.11.001>
- Raso E, Cevasco A, Di Martire D, Pepe G, Scarpellini P, Calcaterra D, Firpo M (2019) Landslide-inventory of the cinque Terre National Park (Italy) and quantitative interaction with the trail network. *J Maps* 15:818–830. <https://doi.org/10.1080/17445647.2019.1657511>

- Riquelme AJ, Abellán A, Tomás R (2015) Discontinuity spacing analysis in rock masses using 3D point clouds. *Eng Geol* 195:185–195. <https://doi.org/10.1016/j.enggeo.2015.06.009>
- Riquelme A, Tomás R, Cano M, Pastor JL, Abellán A (2018) Automatic mapping of discontinuity persistence on rock masses using 3D point clouds. *Rock Mech Rock Eng* 51:3005–3028. <https://doi.org/10.1007/s00603-018-1519-9>
- Robiati C, Eyre M, Vanneschi C, Francioni M, Venn A, Coggan J (2019) Application of remote sensing data for evaluation of Rockfall potential within a quarry slope. *ISPRS Int J Geo Inf* 8(367):1–24. <https://doi.org/10.3390/ijgi8090367>
- Rocscience (2023) RocFall3. Rocscience
- Rodriguez J, Macciotta R, Hendry MT, Roustaei M, Gräpel C, Skirrow R (2020) UAVs for monitoring, investigation, and mitigation design of a rock slope with multiple failure mechanisms—a case study. *Landslides* 17:2027–2040. <https://doi.org/10.1007/s10346-020-01416-4>
- Rossi D, Bigi S, Castello MD, Manna PD (2002) The structure of the Aurunci Mountains (southern Lazio): a balanced cross-section and its restoration. *Boll della Soc Geol Italian* 1:151–159
- Samodra G, Chen G, Sartohadi J et al (2016) Rockfall susceptibility zoning based on back analysis of rockfall deposit inventory in Gunung Kelir, Java. *Landslides* 13:805–819. <https://doi.org/10.1007/s10346-016-0713-7>
- Sarro R, Riquelme A, García-Davalillo JC et al (2018) Rockfall simulation based on UAV photogrammetry data obtained during an emergency declaration: application at a cultural heritage site. *Remote Sens* 10(1923):1–20. <https://doi.org/10.3390/rs10121923>
- Schober A, Bannwart C, Keuschnig M (2012) Rockfall modelling in high alpine terrain – validation and limitations / Steinschlagsimulation in hochalpinem Raum – Validierung und Limitationen. *Geomechan Tunnel* 5:368–378. <https://doi.org/10.1002/geot.201200025>
- Singh B, Goel RK (2011) Strength of discontinuities. In: *Engineering rock mass classification*. Butterworth-Heinemann, Boston, pp 193–204
- Spreafico A, Chiabrando F, Teppati Losè L, Giulio Tonolo F (2021) The iPad pro built-in lidar sensor: 3d rapid mapping tests and quality assessment. *Int Arch Photogramm Remote Sens Spat Inf Sci* 43:63–69. <https://doi.org/10.5194/isprs-archives-XLIII-B1-2021-63-2021>
- Sturzenegger M, Stead D (2009) Close-range terrestrial digital photogrammetry and terrestrial laser scanning for discontinuity characterization on rock cuts. *Eng Geol* 106:163–182. <https://doi.org/10.1016/j.enggeo.2009.03.004>
- Tallini M, Parotto M (2013) Geometry and kinematics of the Montelanico-Carpineto Backthrust (Lepini Mts., Latium) in the hangingwall of the early Messinian thrust front of the central Apennines: implications for the Apennine chain building. *Ital J Geosci* 132:274–289. <https://doi.org/10.3301/IJG.2012.34>
- Tavani S, Billi A, Corradetti A, Mercuri M, Bosman A, Cuffaro M, Seers T, Carminati E (2022) Smartphone assisted fieldwork: towards the digital transition of geoscience fieldwork using LiDAR-equipped iPhones. *Earth Sci Rev* 227(103969):1–15. <https://doi.org/10.1016/j.earscirev.2022.103969>
- Tufano R, Guerriero L, Annibali Corona M, Bausilio G, Di Martire D, Nisio S, Calcaterra D (2022) Anthropogenic sinkholes of the city of Naples, Italy: an update. *Nat Hazards* 112(3):2577–2608. <https://doi.org/10.1007/s11069-022-05279-x>
- Valagussa A, Frattini P, Crosta G, Spizzichino D, Leoni G, Margottini C (2021) Multi-risk analysis on European cultural and natural UNESCO heritage sites. *Nat Hazards* 105:2659–2676. <https://doi.org/10.1007/s11069-020-04417-7>
- Westoby MJ, Brasington J, Glasser NF, Hambrey MJ, Reynolds JM (2012) ‘Structure-from-motion’ photogrammetry: a low-cost, effective tool for geoscience applications. *Geomorphology* 179:300–314. <https://doi.org/10.1016/j.geomorph.2012.08.021>